CHEMICAL ENGINEERING TRANSACTIONS
VOL. 117, 2025
A publication of AIDIC
The Italian Association of Chemical Engineering
Online at www.cetjournal.it
Guest Editors: Fabrizio Bezzo, Flavio Manenti, Gabriele Pannocchia, Almerinda di Benedetto

ISBN 979-12-81206-17-5; **ISSN** 2283-9216
DOI: 10.3303/CET25117130

Experimental Investigation of Hydrodynamics and Mass Transfer in Dense Fluidized Beds

Laura Molignano[a], Maurizio Troiano[a,*], Roberto Solimene[b], Fabrizio Scala[a], Piero Salatino[a]

[a]Dipartimento di Ingegneria Chimica, dei Materiali e della Produzione Industriale, Università degli Studi di Napoli Federico II, Piazzale Vincenzo Tecchio 80, 80125, Napoli, Italy
[b]Istituto di Scienze e Tecnologie per l'Energia e la Mobilità Sostenibili, Consiglio Nazionale delle Ricerche, Piazzale Vincenzo Tecchio 80, 80125, Napoli, Italy
maurizio.troiano@unina.it

The hydrodynamic behaviour of bubbling fluidized beds operated at ambient temperature and at 450 °C is investigated. Geldart B granular solids are fluidized at different gas superficial velocities using a high-pressure drop gas distributor. Customized uncooled capacitance probes are used for the experimental investigation. A statistical analysis of the time series of the local bed voidage is performed, allowing to generate Probability Density Functions (PDF). Emulsion phase features, as voidage and velocity have been estimated, together with visible bubble flow and bubble phase velocity. PDF display multimodal patterns in the part referring to the emulsion phase at increasing gas superficial velocity, highlighting the co-existence of sub-phases characterized by different voidage values. The influence of the bed hydrodynamics and expansion patterns of the emulsion phase on the gas mass transfer around active particles is also investigated. Reactive experiments of catalytic carbon monoxide oxidation are carried out to calculate the particle Sherwood number. Experimental results confirm that a close relationship exists between expansion patterns of the emulsion phase and mass transfer.

1. Introduction

Fluidization technology offers attractive options for efficient thermochemical processing of solid fuels via combustion, gasification, and pyrolysis. Although fluidization technology has been successfully applied to all these processes, there are still broad areas of uncertainties regarding bed hydrodynamics, mixing, and heat and mass transfer phenomena. There is extensive evidence from the literature that fluidization patterns of dense gas fluidized beds may largely depart from the basic two-phase theory (Toomey and Johnstone, 1952). The two-phase theory considers the bed is composed of two main phases, solids-free bubbles and a dense emulsion phase, consisting of a mixture of solid particles and gas. The gas exceeding the incipient fluidization velocity, flows across the bed in the form of bubbles, while the emulsion phase is kept at incipient fluidization. In several cases the two-phase theory overestimates the visible bubble flow (Grace and Clift, 1974). This can be due to an increased velocity of the emulsion phase, departing from incipient velocity conditions as the gas velocity increases (Cui et al., 2000) or to an increase of the gas flow through the bubbles (throughflow component) (Lockett et al., 1967). The distribution of fluidizing gas between the bubble and the emulsion phases, the bubble flow patterns, and the voidage in the emulsion phase deeply affect key fluidization features, like the gas bypass in the emulsion phase, visible bubble flow and bubble velocity, mass transfer around fluidized particles. This has stimulated several studies to detailed diagnosis of fluidization patterns by application of a broad variety of experimental techniques (Aprea et al. (2013), Tramontin Silveira Schaffka et al. (2019)). Recently, Molignano et al. (2023) investigated voidage distribution, visible bubble flow and emulsion phase expansion in bubbling fluidized bed of Geldart's B solids by means of capacitance probes. A thorough hydrodynamic characterization of different Geldart B and D solids has also been carried out (Molignano et al. 2024) in a lab-scale apparatus with low pressure drop gas distribution system.

Paper Received: 22 December 2024; Revised: 8 April 2025; Accepted: 25 May 2025
Please cite this article as: Molignano L., Troiano M., Solimene R., Scala F., Salatino P., 2025, Experimental Investigation of Hydrodynamics and Mass Transfer in Dense Fluidized Beds, Chemical Engineering Transactions, 117, 775-780 DOI:10.3303/CET25117130

In the present study, the same approach previously reported has been used to evaluate the effect of gas distribution on the hydrodynamics and mass transfer of Geldart B solids in dense gas fluidized bed operated at room temperature and 450 °C. Bed voidage distribution and emulsion phase expansion have been obtained using a high pressure drop gas distribution system, while varying the excess gas velocity with respect to minimum fluidization conditions, axial and radial position of the capacitance probes. Dedicated experiments have been also conducted to further investigate the mass transfer coefficient.

2. Experimental

Two types of experiments have been carried out: a) hydrodynamic characterization of the dense fluidized bed using uncooled capacitance probes; b) measurement of the mass transfer coefficient between the bed and active catalyst particles during fast catalytic oxidation of CO.

2.1 Apparatus

A stainless steel column, ID 77.92 mm and 1300 mm high, has been used for all the experiments. The fluidization gas distributor is a 4 mm triangular pitch perforated plate. The average pressure drop across the gas distributor is 1098.78 Pa and its ratio to the pressure drop across the bed is always higher than 30%, in agreement with high pressure drop gas distributors. The windbox is a 225 mm high stainless steel column filled with ceramic rings aimed at gas flow equalization. High temperature operation is carried out using a gas pre-heater and two semi-cylindrical 2.4 kW ceramic ovens with thermal insulation. Bed temperature is controlled by a PID control unit, while gas flow rate is regulated by high-precision digital mass flowmeters/controllers. Eight ports are installed along the column height for pressure/temperature and capacitance measurements. Probes are connected to data acquisition modules and signals are acquired on LABVIEW software. Figure 1 reports the scheme of the apparatus used for hydrodynamic characterization with capacitance probes fluidizing the bed with air. For the experiments of mass transfer, the same apparatus was used. Bottles of high purity N_2, O_2 and N_2-CO mixture (30 %v/v CO) were used for the inlet gas. A L-shape stainless-steel probe is inserted from the top of the column to convey 60 L/h of the exit gas to O_2, CO and CO_2 gas analyzers.

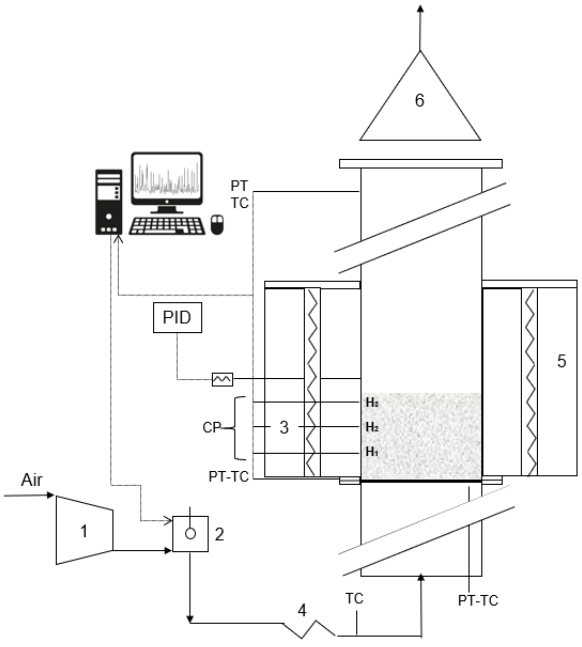

Figure 1: Experimental apparatus. (1) Compressor; (2) air flowmeter; (3) ports for pressure, temperature and capacitance probes; (4) gas pre-heater; (5) electrical furnaces; (6) hood. H_1 = 0.06 m, H_2 = 0.1 m, H_3 = 0.14 m represent the axial distance of the probes from the gas distributor.

2.2 Materials

Grey quartz sand, double sieved in the size range of 0.42-0.59 mm, has been used as bed material. Particle properties are reported in Table 1. For the experiments of mass transfer, a batch of 2% w/w Pt catalyst supported on γ-alumina with an average particle size of 3.9 ± 0.11 mm was mixed in the quartz sand bed.

Table 1: Properties of bed material.

Material	$\overline{d_p}$ $[\mu m]$	ϕ $[-]$	ρ_p $[kg/m^3]$	U_{mf} (20°C) $[m/s]$	U_{mf} (450°C) $[m/s]$	ε_{mf} (20°C) $[-]$	ε_{mf} (450°C) $[-]$	κ_s (20°C) $[-]$	κ_s (450°C) $[-]$
Quartz sand	0.505	0.64	2650	0.196	0.093	0.48	0.49	3.5	6.2

2.3 Diagnostics, experimental procedures and data analysis

Uncooled needle-type capacitance probes have been used for the hydrodynamic characterization of the fluidized bed. The measuring volume of the probe is defined by the electric field, which establishes between the protruding sensor needle and the outer diameter of the ground electrode. The ground tube outer diameter is 6.75 mm, the needle length and diameter are 5.7 mm and 1.6 mm, respectively. The volume of the measured domain can be estimated around 130 mm^3, calculated as mean value of the volume associated to a cylinder and to a cone. More details are provided in Molignano et al. (2023). The bed was fluidized with air at ambient temperature ad at 450 °C. An excess gas superficial velocity in the range 0.005-0.4 m/s was used at room temperature, while values up to 0.7 m/s were reached for experiments at 450 °C, corresponding to freely bubbling fluidization regime. Reactive experiments were carried out at 450 °C. External diffusion around the catalyst particles was considered as the controlling resistance for CO oxidation, as previously verified (Scala, 2007). Superficial gas velocity during reactive experiments was in the range 0.293 – 0.793 m/s, corresponding to freely bubbling fluidization regime. The mass of the catalyst for each velocity condition was chosen so as to have a very low conversion of carbon monoxide, x_{CO}, of about 5 % (i.e. differential conversion conditions). The mass of catalyst particles increased with increasing flowrate due to the decrease of the gas residence time. After catalyst feeding, concentrations of CO, CO_2 and O_2 in the exhaust gases were measured by the analyzers and signals acquired using the LabVIEW software at a sampling rate of 1 Hz during the transient and the steady-state conditions. For the hydrodynamic characterization, time-resolved voltage signals of capacitance probes were first converted into relative dielectric constant of the fluidized medium and then into local bed voidage. Probability Density Functions (PDF) of local bed voidage time series were obtained while varying operating gas velocity, temperature and radial/axial position of the probes (Molignano et al. 2023). For multimodal PDF, deconvolution technique was applied to evaluate the area of each peak in the part of the PDF referring to the emulsion phase. The emulsion phase velocity U_e was calculated according to three different methods: the first one proposed by Hilligardt and Werther (1987) (equation 1) requires the knowledge of U_{mf}; the second one using the Richardson-Zaki correlation (Richardson and Zaki 1954) (equation 2) requires U_{mf} and the voidage of the emulsion phase ε_e; the third one from a gas balance over the cross section of the fluidized bed (equation 3), requires also the estimation of the visible bubble flow from the experiments (bubble velocity U_b and fraction of the bed occupied by bubbles δ).

$$\frac{U_e - U_{mf}}{U - U_{mf}} = {}^1/_3 \tag{1}$$

$$\frac{U_e}{U_{mf}} = \left(\frac{\varepsilon_e}{\varepsilon_{mf}}\right)^n \tag{2}$$

$$U = U_e(1-\delta) + U_b\delta + k_{tf}U_e\delta \tag{3}$$

Details of the three methods are reported elsewhere (Molignano et al. 2024). The time series of the local voidage measured inside the bed have been further analyzed to obtain the visible bubble flow (Fu et al., 2019). For mass transfer experiments in the emulsion phase, the analysis of the data assumes that catalysts particles are in the dense phase of the fluidized bed. Gas in bubble phase is considered in plug flow, while gas and solids in the emulsion phase are well stirred, according to the two-phase fluidization theory. The bubble-emulsion phase mass transfer coefficient is calculated as proposed by Sit and Grace (1981). Sherwood number is defined and calculated as:

$$Sh = \frac{k_g d_a}{\mathfrak{D}_{CO}} = \frac{d_a A_r}{\mathfrak{D}_{CO} A_a} \cdot \frac{U_{mf} + (U - U_{mf})(1 - e^{-X})}{(1 - x_{CO}) - \frac{U - U_{mf}}{U} e^{-X}} x_{CO} \tag{4}$$

3. Results and discussion

3.1 Hydrodynamic characterization

Figure 2 reports PDF of local voidage at ambient temperature and at 450 °C, with capacitance probe located, as reference, at height H_2, while varying excess gas velocity and radial coordinate of the probe. Regardless the operating temperature, at low excess gas velocity, close to minimum fluidization conditions, the PDF has a unimodal trend, with a sharp peak for voidage modal values close to minimum fluidization voidage. The bed is mainly composed by the emulsion phase, with some small bubbles with high voidage contributing to the tail of PDF. At higher excess gas superficial velocities, a bimodal nature of the PDF is evident in the component associated to the emulsion phase: a lower voidage LV-phase and a higher voidage HV-phase co-exist. This behaviour is accentuated at high temperature with bimodal PDF referred to the emulsion phase appearing at lower excess gas velocities. Furthermore, at high temperature higher values of voidage referred to the emulsion phase are obtained and more pronounced peaks related to bubble phase are evident in Figure 2. These results, typical of freely bubbling fluidization regime, are in good agreement with previous results obtained with the same solid material, using a low pressure drop gas distributor (Molignano et al., 2023).

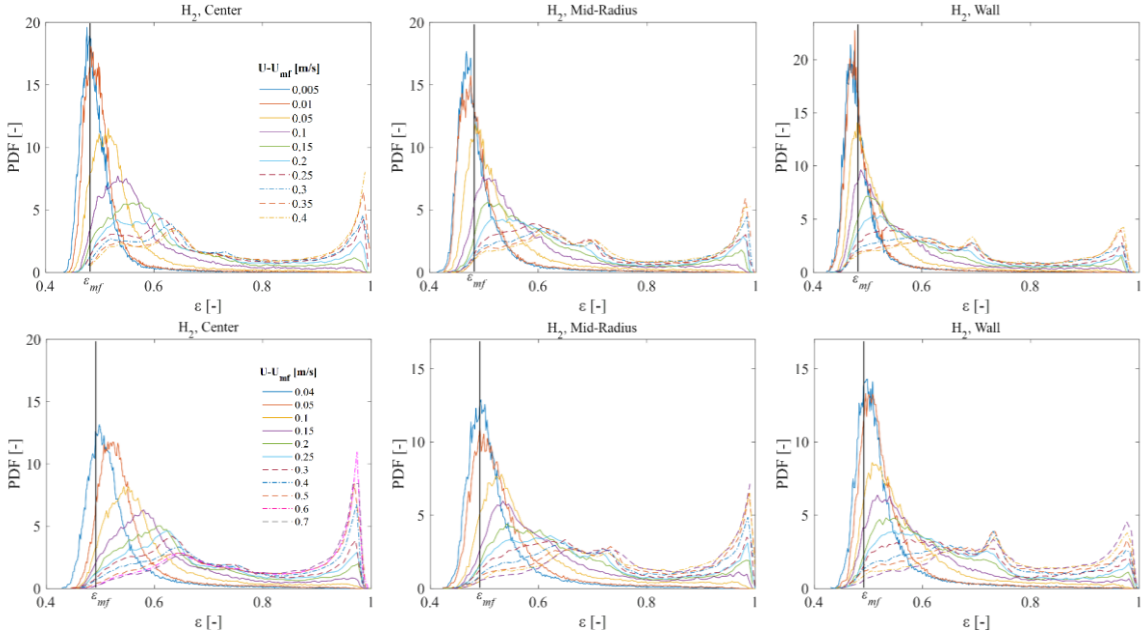

Figure 2: Probability density functions of the local voidage at ambient temperature (top) and at 450 °C (down) for different $U - U_{mf}$ and probe locations.

Figure 3a reports the values of voidage associated to the emulsion phase for each PDF at probe height H_2, while varying excess gas velocity and radial position of the probe at 450 °C. For gas excess higher than 0.1 – 0.15 m/s a bimodal character of voidage distribution is evident, regardless the radial coordinate of the probe.

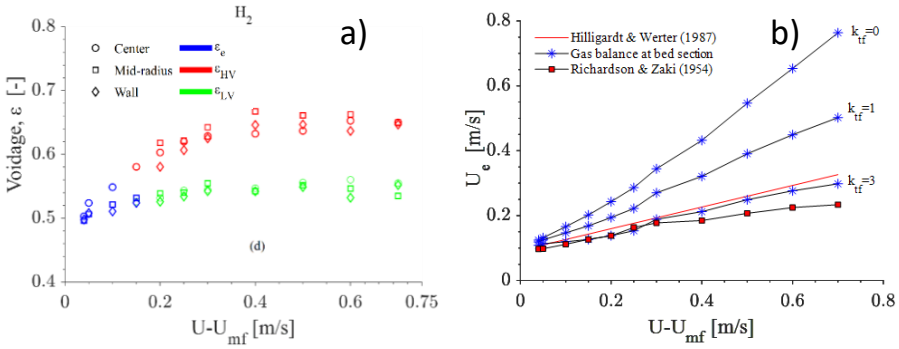

Figure 3: Hydrodynamic characterization results at 450 °C for different $U - U_{mf}$ and probe radial coordinates at H_2. Emulsion phase voidages (3a); emulsion phase velocity (3b).

Figure 3b reports the trend of the emulsion phase velocity U_e obtained by the three different methods explained above, while varying the excess gas velocity. The value of U_e from the gas mass balance is reported for three values of the throughflow coefficient k_{tf}, namely 0, 1 and 3. k_{tf}=0 means no gas through bubbles, while k_{tf}=3 corresponds to isolated and spherical bubbles (Gilliland 1963). From Figure 3b, it is evident that the three methods give similar results, if a k_{tf} =3 is used in the mass balance. This result suggests that for the investigated gas distribution conditions, bubbles are characterized by slow motion and small initial size. These results confirm the validity of the Richardson-Zaki correlation during aggregative fluidization in the evaluation of the emulsion phase expansion and velocity.

3.2 Mass transfer in the emulsion phase

Figure 4 reports Sherwood number obtained from the experiments, while varying the excess gas velocity. Sherwood numbers estimated using a Frössling-type correlation in which the emulsion phase velocity U_e is evaluated from the three methods cited above (Figure 3b) are also reported. Equation 5 reports the Frössling-type expression used in the present work:

$$Sh = 2 * \varepsilon + K\left(\frac{Re}{\varepsilon}\right)^{0.5} * Sc^{\frac{1}{3}} \qquad K=0.7 \tag{5}$$

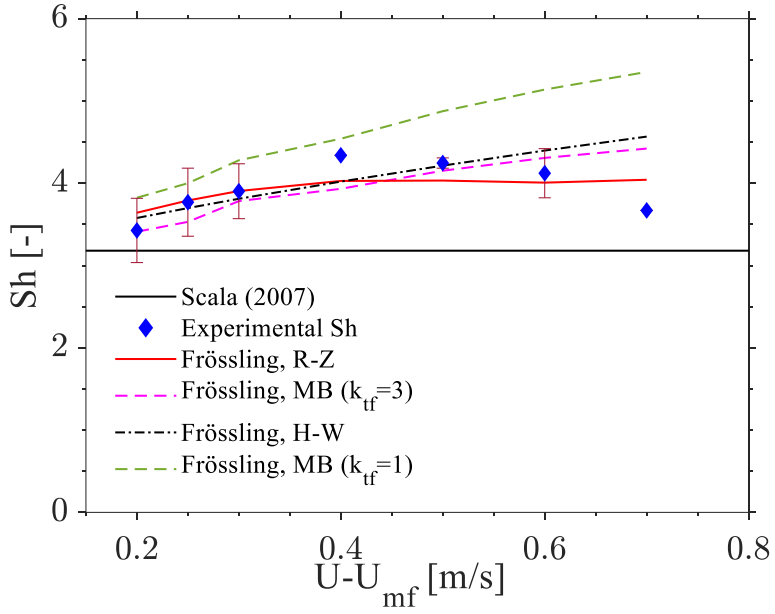

Figure 4: Sherwood number as a function of excess gas superficial velocity. T=450 °C.

Red curve in Figure 4 reports Sh estimated by Frössling expression with section-averaged HV voidage at height H_2 and U_e from Richardson-Zaki correlation. Dashed pink curve is obtained by using Frössling expression with section-averaged HV voidage at height H_2 and U_e from gas mass balance with k_{tf}=3, while green curve is obtained with k_{tf}=1. Black dashed-dotted curve is obtained by Frössling expression with section-averaged HV voidage at height H_2 and U_e from Hilligardt and Werther correlation. Black continuous curve is obtained considering both the emulsion voidage and velocity at minimum fluidization conditions. Experimental Sh numbers first increase with the excess gas velocity and then keep a nearly constant value. Experimental Sh values are in agreement with Frössling expression calculated with Richardson-Zaki correlation and with mass balance for k_{tf}=3. If the present Sh numbers are compared to those achieved under hydrodynamic conditions obtained with low pressure drop distributor (Molignano et al., 2023), Sh decreases for high pressure drop distributor. It is likely that the high pressure drop distributor determines smaller and more isolated bubbles reducing the shear in the emulsion phase and, in turn, the mass transfer coefficient.

4. Conclusions

The hydrodynamics of dense fluidized beds of groups B solids, operated at ambient temperature and 450 °C, has been successfully characterized using capacitance probes. Probability density functions display a unimodal character at low gas velocities, while a bimodal character associated to the emulsion phase of the bed is

obtained, which is more pronounced as the gas superficial velocity is increased. Higher-voidage phase is dominant (0.6-0.68), especially at high gas excess velocities (>0.2m/s), and it can be used to estimate the emulsion phase velocity (0.1-0.8m/s) and to evaluate gas-solids mass transfer in fluidized beds (Sh=3.5-4.5). The gas distributor affects the main hydrodynamic features in terms of voidage, visible bubble flow, emulsion phase velocity and, consequently, the mass transfer. These aspects are crucial for the design and operation of many processes aimed at thermochemical conversion of solid fuels in fluidized beds.

Nomenclature

A_a – active particle surface area, m^2
A_r – reactor cross-section area, m^2
d_a – active particle diameter, m
$\mathfrak{D}_{CO}$ – diffusion coefficient CO, m^2/s
$\overline{d_p}$ – average particle size, m
H_2 – axial coordinate, m
k_g – gas mass transfer coefficient, m/s
k_s – solids dielectric constant, -
k_{tf} – throughflow coefficient, -
n – parameter in RZ correlation, -
Sh – Sherwood number, -
U – superficial gas velocity, m/s
U_b – bubble velocity, m/s
U_e – emulsion phase velocity, m/s
U_{mf} – minimum fluidization velocity, m/s
X – bubble-emulsion phase mass transfer index, -
x_{CO} – CO conversion, -
δ – bubble fraction, -
ε – voidage, -
ε_e – emulsion phase voidage, -
ε_{mf} – voidage at minimum fluidization conditions, -
ρ_p – particle density, kg/m^3
ϕ – sphericity, -
ρ_p – particle density, kg/m^3

Acknowledgments

The authors gratefully acknowledge Mr. Antonio Cammarota for the set-up of the experimental apparatus, and Mr. Antonio Russo, University of Naples, for the support during the experimental campaign.

References

Toomey R.D., Johnstone H.F., 1952, Gaseous fluidization of solid particles, Chemical Engineering Progress, 48, 220–226.
Fu Z., Zhu J., Barghi S., Zhao Y., Luo Z., Duan C., 2019, On the two-phase theory of fluidization for Geldart B and D particles, Powder Technology, 354, 64–70.
Cui H., Mostoufi N., Chaouki J., 2000, Characterization of dynamic gas-solid distribution in fluidized beds, Chemical Engineering Journal, 79, 133–143.
Grace J.R., Clift R., 1974, On the two-phase theory of fluidization, Chemical Engineering Science, 29, 327–334.
Lockett M.J., Davidson J.F., Harrison D., 1967, On the two-phase theory of fluidization, Chemical Engineering Science, 22, 1059–1066.
Aprea G., Cammarota A., Chirone R., Solimene R., Salatino P., 2013, Hydrodynamic Characterization of the Biomass Combustion in a Pilot Scale Fluidized Bed Combustor, Chemical Engineering Transactions, 32, 1519–1524.
Tramontin Silveira Schaffka F., Jairo Ramirez Behainne J., Parise M.R., Castilho G.J., 2019, Effect of the Solids Inventory and Fluidization Gas Velocity on the Hydrodynamics of a Circulating Fluidized Bed, Chemical Engineering Transactions, 74, 1009–1014.
Molignano L., Troiano M., Solimene R., Tebianian S., Scala F., Salatino P., Joly J.F., 2023, Hydrodynamics and mass transfer around active particles in dense gas-fluidized beds, Fuel, 341, 127590.
Molignano L., Troiano M., Solimene R., Tebianian S., Joly J.F., Salatino P., 2024, Exploring the hydrodynamics of dense beds of Geldart B and D gas-fluidized particles through the analysis of capacitance probe signals, Powder Technology, 447, 120174.
Scala F., 2007, Mass transfer around freely moving active particles in the dense phase of a gas fluidized bed on inert particles, Chemical Engineering Science, 62, 4159–4176.
Sit S.P., Grace J.R., 1981, Effect of bubble interaction on interphase mass transfer in gas fluidized beds, Chemical Engineering Science, 36, 327–335.
Hilligardt K., Werther J., 1987, Influence of temperature and properties of solids on the size and growth of bubbles in gas fluidized beds, Chemical Engineering & Technology, 10, 272–280.
Gilliland E.R., 1963, Fluidised particles, Davidson J.F. and Harrison D., Cambridge University Press, New York.
Richardson J.F., Zaki W.N., 1954, Sedimentation and fluidisation. Part 1, Transactions of the Institution of Chemical Engineers, 32, 35–53.